REPORT DOCUMENTATION PAGE	*Form Approved* *OMB No. 0704-0188*

1. REPORT DATE *(DD-MM-YYYY)* 21-10-2013	**2. REPORT TYPE** Journal Article	**3. DATES COVERED** *(From - To)*

4. TITLE AND SUBTITLE Strontium Concentrations in Corrosion Products from Residential Drinking Water Distribution Systems	**5a. CONTRACT NUMBER** **5b. GRANT NUMBER** **5c. PROGRAM ELEMENT NUMBER** 0601153N
6. AUTHOR(S) Tammie L. Gerke, Brenda J. Little, Todd P. Luxton, Kirk G. Scheckel and J. Barry Maynard	**5d. PROJECT NUMBER** **5e. TASK NUMBER** **5f. WORK UNIT NUMBER** 73-4635-02-5
7. PERFORMING ORGANIZATION NAME(S) AND ADDRESS(ES) Naval Research Laboratory Oceanography Division Stennis Space Center, MS 39529-5004	**8. PERFORMING ORGANIZATION REPORT NUMBER** NRL/JA/7303--12-1210
9. SPONSORING/MONITORING AGENCY NAME(S) AND ADDRESS(ES) Office of Naval Research One Liberty Center 875 North Randolph Street, Suite 1425 Arlington, VA 22203-1995	**10. SPONSOR/MONITOR'S ACRONYM(S)** ONR **11. SPONSOR/MONITOR'S REPORT NUMBER(S)**

12. DISTRIBUTION/AVAILABILITY STATEMENT

Approved for public release, distribution is unlimited.

13. SUPPLEMENTARY NOTES

14. ABSTRACT

The United States Environmental Protection Agency (US EPA) will require some U.S. drinking water distribution systems (DWDS) to monitor nonradioactive strontium (Sr2+) in drinking water in 2013. Iron corrosion products from four DWDS were examined to assess the potential for Sr2+ binding and release. Average Sr2+ concentrations in the outermost layer of the corrosion products ranged from 3 to 54 mg kg -1 and the Sr2 + drinking water concentrations were all ≤0.3 mg L -1. Micro-X-ray adsorption near edge structure spectroscopy and linear combination fitting determined that Sr2+ was principally associated with CaCO3. Sr2+ was also detected as a surface complex associated with α-FeOOH. Iron particulates deposited on a filter inside a home had an average Sr2+ concentration of 40.3 mg kg -1 and the associated drinking water at a tap was 210 μg L -1. The data suggest that elevated Sr2+ concentrations may be associated with iron corrosion products that, if disturbed, could increase Sr2+ concentrations above the 0.3 μg L -1 US EPA reporting threshold. Disassociation of very small particulates could result in drinking water Sr2+ concentrations that exceed the US EPA health reference limit (4.20 mg kg -1 body weight).

15. SUBJECT TERMS

iron, drinking water, strontium

16. SECURITY CLASSIFICATION OF:			**17. LIMITATION OF ABSTRACT**	**18. NUMBER OF PAGES**	**19a. NAME OF RESPONSIBLE PERSON**
a. REPORT	**b. ABSTRACT**	**c. THIS PAGE**			Brenda Little
Unclassified	Unclassified	Unclassified	UU	7	**19b. TELEPHONE NUMBER** *(Include area code)* (228) 688-5494

Reset

Environmental Science & Technology
Article
pubs.acs.org/est

Strontium Concentrations in Corrosion Products from Residential Drinking Water Distribution Systems

Tammie L. Gerke,*[†] Brenda J. Little,[‡] Todd P. Luxton,[§] Kirk G. Scheckel,[§] and J. Barry Maynard[†]

[†]Department of Geology, University of Cincinnati, Cincinnati, Ohio 45221-0013, United States
[‡]Naval Research Laboratory, Stennis Space Center, Mississippi 39529, United States
[§]U.S. Environmental Protection Agency, ORD, NRMRL, LRPCD, Cincinnati, Ohio 45268, United States

S Supporting Information

ABSTRACT: The United States Environmental Protection Agency (US EPA) will require some U.S. drinking water distribution systems (DWDS) to monitor nonradioactive strontium (Sr^{2+}) in drinking water in 2013. Iron corrosion products from four DWDS were examined to assess the potential for Sr^{2+} binding and release. Average Sr^{2+} concentrations in the outermost layer of the corrosion products ranged from 3 to 54 mg kg^{-1} and the Sr^{2+} drinking water concentrations were all ≤0.3 mg L^{-1}. Micro-X-ray adsorption near edge structure spectroscopy and linear combination fitting determined that Sr^{2+} was principally associated with $CaCO_3$. Sr^{2+} was also detected as a surface complex associated with α-FeOOH. Iron particulates deposited on a filter inside a home had an average Sr^{2+} concentration of 40.3 mg kg^{-1} and the associated drinking water at a tap was 210 μg L^{-1}. The data suggest that elevated Sr^{2+} concentrations may be associated with iron corrosion products that, if disturbed, could increase Sr^{2+} concentrations above the 0.3 μg L^{-1} US EPA reporting threshold. Disassociation of very small particulates could result in drinking water Sr^{2+} concentrations that exceed the US EPA health reference limit (4.20 mg kg^{-1} body weight).

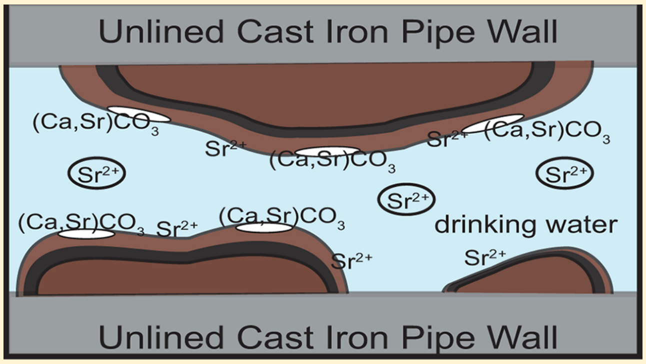

INTRODUCTION

Strontium (Sr^{2+}, atomic number 38), highly mobile and reactive, is estimated to be the fifteenth most abundant element on Earth. It has four naturally occurring stable isotopes, ^{84}Sr, ^{86}Sr, ^{87}Sr, and ^{88}Sr, and 31 unstable ones. The longest-lived unstable isotope is ^{90}Sr with a half-life of 28.9 years. Strontium is only found naturally in compounds and has an atomic radius similar to calcium (Ca^{2+}). Strontium readily substitutes for Ca^{2+} in the metal site (M1) of minerals and in the structure of bone.[1] The most common Sr^{2+} compounds are $Sr^{2+}SO_4$ (celestite) and $Sr^{2+}CO_3$ (strontianite).

Naturally occurring Sr^{2+} compounds are highly soluble in water; consequently, Sr^{2+} is readily released into ground and surface waters that are sources for drinking water. Ingestion of nonradioactive Sr^{2+} has been considered a potential threat to human health in recent years.[2−5] Based on that potential, the US EPA listed Sr^{2+} on the Drinking Water Contaminant Candidate List 3 (CCL3[6]). If approved, CCL3, will result in regulatory limits for Sr^{2+} concentrations in drinking water.

In May 2012, the Director of the US EPA signed the Unregulated Contaminant Monitoring Rule 3, which includes Sr^{2+} (UCMR3[7]). The UCMR3 requires that samples of drinking water be collected at the point-of-entry into and at the point-of-maximum residence time in a DWDS. These locations were chosen because water chemistry and quality are changeable as drinking water travels through and interacts with the DWDS infrastructure and associated corrosion products.[7,8] Starting in 2013, reporting to the US EPA is required if the Sr^{2+} water concentration exceeds 0.3 μg L^{-1} at either location in the DWDS. Average Sr^{2+} concentration in United States drinking water is approximately 1.1 mg L^{-1}.[5,9,10] Therefore, it is likely that the drinking water of numerous DWDS will exceed 0.3 μg L^{-1}.

Surface layers of iron corrosion products act as sinks for metal ions and oxyanions.[11,12] Potential concentrations of Sr^{2+} and mechanism(s) of inclusion are currently unknown. If Sr^{2+} does accumulate in iron corrosion products and they are disturbed, either hydraulically or chemically, pulses of elevated Sr^{2+} concentrations in the water or Sr^{2+}-rich particulates could reach the consumer tap.[12,13]

Data on Sr^{2+} concentrations, methods of binding, and adsorption are needed to assess mechanisms of release and ultimately the potential impact to human health. The objective of the current study was to determine the abundance, distribution, and bonding mechanisms of Sr^{2+} in surface layers of iron corrosion products from unlined cast iron and galvanized iron drinking water pipes. In addition to traditional

Received: January 7, 2013
Revised: April 16, 2013
Accepted: April 19, 2013
Published: April 22, 2013

ACS Publications

dx.doi.org/10.1021/es4000609 | *Environ. Sci. Technol.* 2013, 47, 5171−5177

physiochemical characterization techniques, Sr^{2+} binding mechanisms within the corrosion products were examined using *in situ* micro X-ray adsorption near edge spectroscopy (μ-XANES). The amount of Sr^{2+} that could potentially be reintroduced into drinking water from iron corrosion products was examined using particulates collected at the point-of-entry into a consumer home.

EXPERIMENTAL SECTION

Iron Corrosion Product Sample Collection and Preparation. Mound-shaped iron corrosion products were obtained from pipe samples of four fully operational DWDS. Eighteen iron corrosion products were harvested from subsections of a highly corroded 8.5 m long 10 cm inner diameter (id) unlined cast iron residential main from Utility A (UA). Two representative samples from Utility B (UB) and one from Utility C (UC) were collected from single 30 cm long sections of 15 cm id unlined cast iron residential mains. Two iron corrosion products from Utility D (UD) were harvested from a 30 cm long section of a 2.54 cm id galvanized iron riser pipe. While in service, all sections were exposed to daily periods of stagnation. Pipes, obtained as a result of pipe failures or replacements, were transported to the laboratory. All were cut longitudinally with a saw, allowed to air-dry for up to 72 h, and imaged using a Canon G3 digital camera.

Subsamples (up to 3.0 g) were obtained from regions within the mounds (i.e., core, shell and surface layers (Sarin et al.[14]) (Figure 1)), using brushes and metal spatulas to minimize cross-contamination between layers. Colors for each layer were determined by comparison to a standard color chart (Cornell and Schwertmann[15]). Material was ground by hand with an agate mortar and pestle and aliquots were used for mineralogical and chemical analyses. Approximately 0.25 g of each region was thoroughly mixed with 2.25 g of cellulose and pressed into 31 mm pellets for X-ray fluorescence (XRF) analysis.

Figure 1. Image of a 25 cm long sediment filter and XRF disks from a home in Utility A. Filter was in use for four years.

Two representative iron corrosion products from UA (samples UA11 and UA13; Table S1, Supporting Information) and one from UB (UB1; Table S1, Supporting Information) were used for synchrotron-based, in situ μ-XANES analysis. A 1-cm long section of each sample was encased in Buehler EpoThin low viscosity epoxy and a subsample of each was cut to include core, shell, and surface layers. One side of each sample was polished and photographed using a Canon G3 digital camera. Images were used to determine locations for μ-XANES analyses.

Sediment Filter Collection and Preparation. A 25 cm long polypropylene sediment filter (retains particles >5 μ) in use for four years (2008 to 2012) was removed from a residence, transported to the laboratory, and air-dried. The filter was cut longitudinally and laterally (Figure 1) and two 12.5 cm long strips were removed from the outer wall. Strips were placed in sterile beakers and heated to 200 °C for 1 h, melting the filter material and creating disks that were used for XRF analysis (Figure 1). Heating did not alter the concentrations of metals of interest.

Water Chemistry. Surface waters are used as source waters for all four utilities. The disinfection used in UA and UC is free chlorine and for UB and UD, chloramine. Table 1 lists water quality parameters for treated water from each utility including Sr^{2+} concentrations.

Table 1. Selected Water Quality Parameters of Finished Drinking Waters for the Four Drinking Water Distribution Systems That Samples for This Study Were Obtained

	utility			
param.	A	B	C	D
pH	8.6	7.78	8.14−8.54	7.26−7.69
hardness (mg L^{-1} as $CaCO_3$)	91−177	137	NR[a]	91−196
alkalinity (mg L^{-1} as $CaCO_3$)	68	112	23.3−27.3	37−111
Ca (average)	36	–[b]	NR	NR
chlorine, free (mg L^{-1})	0.97	–	0.04−2.03	–
chlorine, total (mg L^{-1})	NR	NR	NR	0.0−4.3
NH_2Cl (mg L^{-1})	–	1.22	–	–
chlorine dioxide (μg L^{-1})	–	–	40−760	–
orthophosphate (mg-PO_4 L^{-1})	–	0.5	NR	2.1−3.0
phosphate (mg-PO_4 L^{-1})	0.083	–	NR	–
Sr^{2+} (μg L^{-1})	300	110[c]	<0.1	164−173

[a]NR = not reported if used in the treatment process. [b]– = not applicable. [c]Ref 48.

Bulk Sample Analytical Methods. *Powder X-ray Diffraction (XRD).* Samples were analyzed using a Siemens D-500 automated diffractometer system equipped with a Cu Kα tube set at 30 mA and 40 kV (Department of Geology, University of Cincinnati, Cincinnati, OH). The 2θ ranged from 5 to 60 or 70. Regardless of the 2θ range, a 0.02° step size and a 2 s count time was used at each step. Crystalline phases were identified following the protocol of Gerke et al.[12] Mineralogical analyses were conducted to determine the iron phases that formed as Fe, released as a result of corrosion, interacted with bulk water. Accessory phases, defined as phases that precipitate from the bulk water (e.g., $CaCO_3$, calcite) or phases that are transported from upstream in the DWDS (e.g., SiO_2, quartz), were also identified. The detection limit for most mineral phases is 5 to 10%.

Bulk X-ray Fluorescence. Pressed pellets and sediment filter disks were analyzed for major oxides and trace elements using a Rigaku 3070 X-ray fluorescence spectrometer (Department of Geology, University of Cincinnati, Cincinnati, OH). Intensity data were converted to percent (by weight) or mg kg^{-1} following the protocol of Gerke et al.[12]

Synchrotron Bulk and μ-X-ray Absorption Near Edge Structure (bulk and μ-XANES) Run Conditions and Analysis. X-ray μ-beam studies were performed at beamline XOR/PNC 20 μ_B-B [16] and MRCAT Sector 10[17,18] of the Advanced Photon Source (APS), Argonne National Laboratory (Argonne, IL) in top-up mode at 7 GeV and a ring current of 101 mA. A 0.5 mm premonochromator slit width and a Si(111) double crystal monochromator detuned by 10% to reject higher-order harmonics was used at both beamlines. The monochromator beam energy position at both beamlines was calibrated by assigning the first inflection of the absorption edge of Sr^{2+} to 16105 eV following the protocol of O'Day et al.[19]

Three Sr *K*-edge μ-XANES scans were collected at ambient temperature in fluorescence mode with a solid-state 13-element Ge solid-state Canaberra detector for samples UA11 and UA13 at beamline XOR/PNC 20 μ_B-B. Six Sr *K*-edge XANES scans were collected at ambient temperature in fluorescence mode with a solid-state 4-element Si-drift detector for sample UB1 at beamline MR-CAT 10-ID.

Bulk XANES scans of the Sr standards were collected at both beamlines. Standards included Sr^{2+} adsorbed to α-FeOOH (goethite), γ-FeOOH (lepidocrocite), Fe_3O_4 (magnetite), and $CaCO_3$ (see the Supporting Information for details). A $(Sr,Ca)CO_3$ standard spectrum was obtained from the Lylte database (http://ixs.iit.edu/database/). All spectra were placed on the same energy grid and aligned to $SrCl_2$ (99.99%, Fisher Scientific, Pittsburgh, PA) at 16105 eV, averaged, normalized, and the background removed by spline fitting using IFEFFIT.[20]

Linear combination fitting (LCF) was conducted on the first derivative of the normalized (E) XANES spectra of the standards and samples. Levenberg−Marquardt least-squares algorithm was applied to a fit range of −20 to 80 eV. Each LCF analysis encompassed 124 to 147 data points of a given sample spectrum and all five standard spectra. Best-fit scenarios were defined as having the smallest residual error and the sum of all fractions was close to 1. To fully describe any particular sample within 1% reproducible error, a minimum of two components was necessary, and results have a ± 10% accuracy.

RESULTS

Physicochemical Characterization of Iron Corrosion Products. The 23 representative iron corrosion products had mound-shaped morphologies. The internal structure of each consisted primarily of a core, shell, and surface layer (Figure 2).[14] Some samples had black veins in the core giving them a marbled appearance (Figure 2).[21]

In general, the color for the core region of the UA samples was yellowish-red brown, consisting primarily of α-FeOOH and γ-FeOOH with minor amounts of Fe_3O_4 and the accessory phase $CaCO_3$. Black nonmetallic luster veins were Fe_3O_4 with equal but lesser amounts of α-FeOOH and γ-FeOOH. Shell layers, separating core and surface layers, had black metallic lusters and were primarily Fe_3O_4, with lesser amounts of α-FeOOH and γ-FeOOH and trace amounts of the accessory phase $CaCO_3$. Surface layers, reddish-brown in color, were composed of nearly equal amounts of α-FeOOH and γ-FeOOH, lesser amounts of Fe_3O_4 and trace amounts of the accessory phases SiO_2 and $CaCO_3$. (Figure 3a) (Figure S1, Supporting Information)

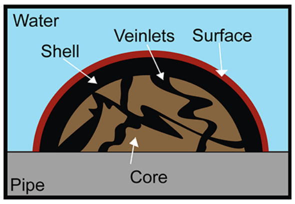

Figure 2. Schematic of the idealized internal structure of a mound-shaped iron drinking water pipe corrosion product (after refs 14, 21, and 47).

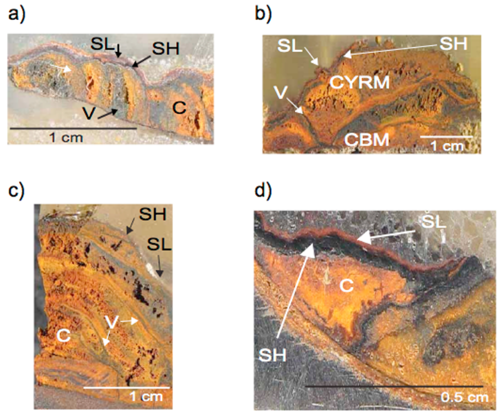

Figure 3. Digital images of a cross-section of representative iron corrosion products from (a) Utility A, (b) Utility B, (c) Utility C, and (d) Utility D. The C (core), CYRM (core-yellowish-red brown material), CBM (core-black material), V (veins), SH (shell layer) and SL (surface layer) are indicated in the cross-section images. The scales are in cm.

Samples from UB were similar with yellowish-brown cores consisting of equal amounts of α-FeOOH and γ-FeOOH and traces of Fe_3O_4. In sample UB2 portions of the core were composed of black nonmetallic luster Fe_3O_4 and lesser amounts of α-FeOOH and γ-FeOOH. Shell layers were discontinuous with a black metallic luster consisting of equal amounts of α-FeOOH and γ-FeOOH and trace amounts of Fe_3O_4. Discontinuous surface layers, reddish-brown in color, contained similar amounts of α-FeOOH and γ-FeOOH and varying amounts of Fe_3O_4 but always less than the iron oxyhydroxides. (Figure 3b) (Figure S2, Supporting Information)

The UC sample, previously described by Gerke et al.,[22] had a yellowish-red brown α-FeOOH-rich core with lesser amounts of Fe_3O_4 and trace amounts of the accessory phase $CaCO_3$. Nonmetallic luster black veins, present throughout the core, were Fe_3O_4 with minor amounts of α-FeOOH. The core was capped by a black metallic shell layer of Fe_3O_4 with trace amounts of α-FeOOH and moderate amounts of the accessory phase $CaCO_3$. The surface layer was discontinuous, yellowish-red brown and consisted of nearly equal amounts of γ-FeOOH and Fe_3O_4 and trace amounts of α-FeOOH. Three accessory phases were identified in the surface layers: SiO_2, $CaCO_3$, and S (sulfur) (Figure 3c) (Figure S3, Supporting Information).

Samples from UD were also previously described.[12] Yellowish-brown core regions were primarily α-FeOOH with trace amounts of the accessory phase SiO_2. Shell layers were mainly Fe_3O_4 and some also contained α-FeOOH. The reddish-brown

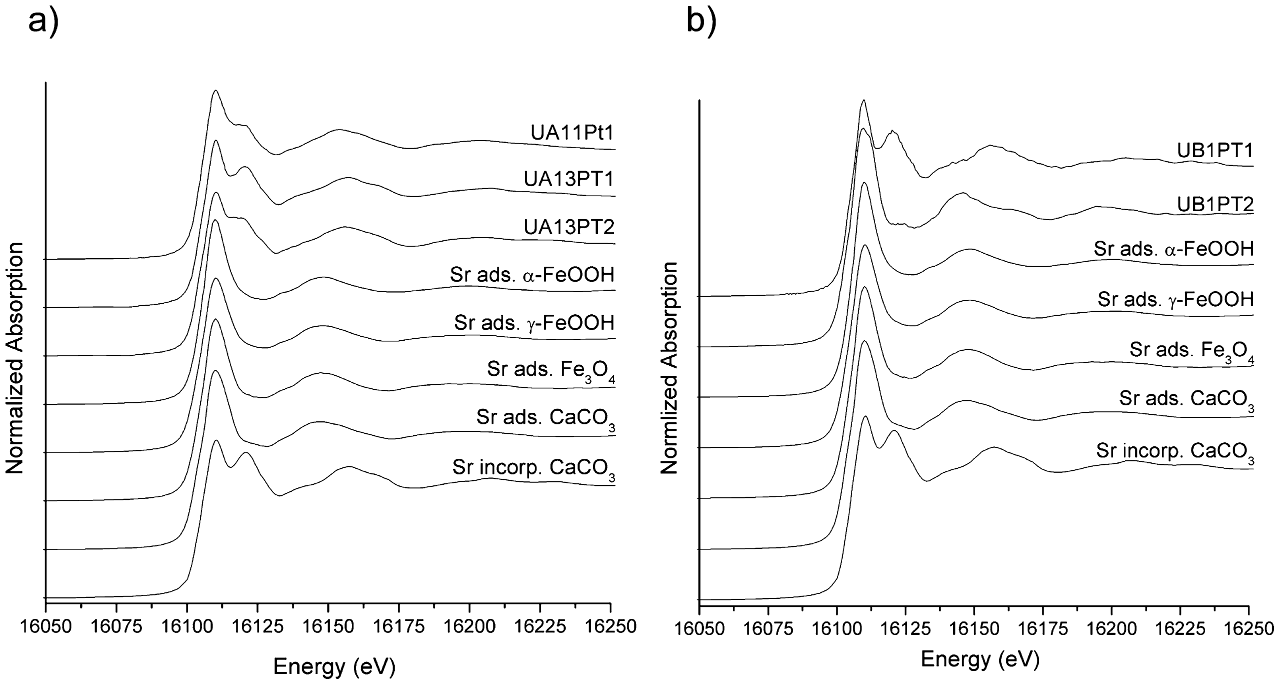

Figure 4. Strontium *K*-edge for bulk XANES Sr^{2+} standards spectra and the in situ μ-XANES for samples (a) UA11 point 1 (UA11PT1) and UA13 points 1 and 2 (UA13PT1, and UA13PT2 and (b) UB1 point 1 and 2 (UB1PT1 and UB1PT2). The Sr^{2+} standards are $CaCO_3$ in which some of the Ca^{2+} sites have been filled with Sr^{2+} (Sr^{2+} incorp. $CaCO_3$) and Sr^{2+} adsorbed to; α-FeOOH (Sr^{2+} ads. α-FeOOH), γ-FeOOH (Sr^{2+} ads. γ-FeOOH), Fe_3O_4 (Sr^{2+} ads. Fe_3O_4), and $CaCO_3$ (Sr^{2+} ads. $CaCO_3$).

surface layers were primarily α-FeOOH. The surface layer of Sample UD1 had lesser amounts of Fe_3O_4 (Figure 3d).[12]

Concentration of Sr^{2+} in the Drinking Water, Iron Corrosion Products from All Four Utilities, and Sediment Filter Particulates. Strontium concentrations in the surface layers of the iron corrosion products for all utilities ranged from 3 to 128 mg kg^{-1} (Table S1, Supporting Information). The average Sr^{2+} concentration in solids compared to water at the point of entry for the utilities were as follows: Utility A, 38 mg kg^{-1} and 0.3 mg L^{-1}; Utility C, 3 mg kg^{-1} and water at point-of-entry was below the detection limit; Utility D, 54 mg kg^{-1} and 0.167 to 0.174 mg L^{-1} (Table 1). The average concentration in solids from Utility B average was 12 mg kg^{-1} and the concentration in water at the point of entry was assumed to be 0.110 mg kg^{-1}. The Sr^{2+} concentrations of the sediment filter particulates from a residence served by UA ranged from 39.74 to 40.77 mg kg^{-1}, with an average of 40.26 mg kg^{-1} (Table S1, Supporting Information). Data for all regions of the mound-shaped corrosion products and the iron particulate sediment filter samples are provided in Table S1, Supporting Information.

Adsorption Mechanism of Sr^{2+} with Iron Corrosion Products. Sr^{2+} *K*-edge in situ μ-XANES spectra from samples UA11 (one spectrum), UA13 (two spectra), and UB1 (two spectra) and bulk XANES spectra for Sr^{2+}-Fe and Sr^{2+}-Ca standards are shown in Figure 4. The Sr^{2+} *K*-edge in situ μ-XANES spectra for UA11 Point 1, UA13 Points 1 and 2, and UB1 Point 1 had prominent peaks at 16110, 16120, and 16156 eV (Figure 4). The μ-XANES spectrum for UB1 Point 2 had pronounced peaks at 16110 and 16146 eV (Figure 4b). The energies of the predominant sample peaks corresponded to characteristic peaks of the standards (Table 2).

Linear combination fit spectra, generated using all standards and the μ-XANES spectrum of a given sample, were superimposed on the first derivative spectrum of UA11, UA13, and UB1, respectively (Figure 5). 60 to 93% of the Sr^{2+} was associated or bound in $CaCO_3$ (Table 3). The highest percentage of Sr^{2+} associated with $CaCO_3$ was found with sample UB1. The remaining Sr^{2+} in the surface layers was associated with α-FeOOH (7 to 39%) (Table 3). Sample UA11 Point 1 had the highest percentage of Sr^{2+} adsorbed to α-FeOOH.

Table 2. Strontium *K*-edge μ-XANES Characteristic Peak Energies for the Five Sr^{2+} Standards

	characteristic peaks (eV)			
standard	16110.6	16120	16148	16156.2
Sr^{2+} ads. α-FeOOH	X		X	
Sr^{2+} ads. γ-FeOOH	X		X	
Sr^{2+} ads. Fe_3O_4	X		X	
Sr^{2+} ads. $CaCO_3$	X		X	
Sr^{2+} incorp. $CaCO_3$	X	X		X

■ DISCUSSION

Iron drinking water pipes corrode producing large amounts of corrosion products that line the internal surfaces of pipe walls.[23−26] Corrosion products are demonstrated sinks for metal ions, including vanadium, arsenic, chromium, copper, and lead.[11,12] It is reasonable to hypothesize that Sr^{2+} also concentrates in the surface layers of iron drinking water pipe corrosion products.

Ingestion of Sr^{2+} from drinking water has become such a concern that in May 2012 the US EPA director signed the UCMR3 that requires monitoring of Sr^{2+} in drinking water. The UCMR3 specifically states that incorporation of cobalt and/or strontium into pipe deposits within a distribution system could result in mobilization of these metals into

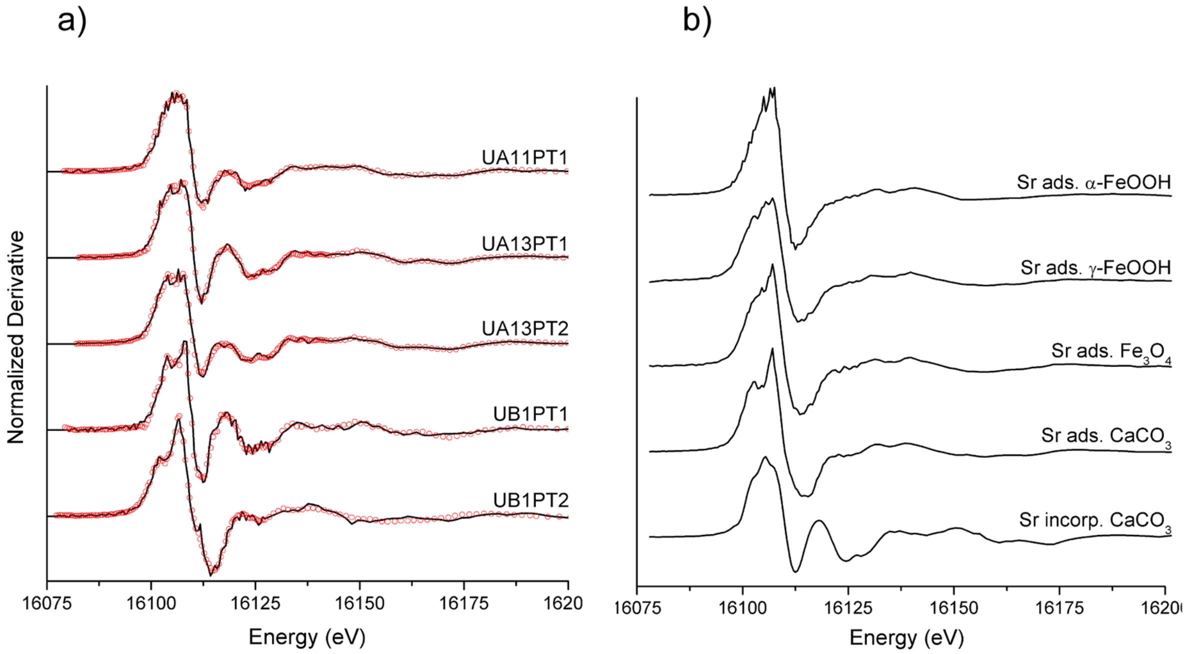

Figure 5. (a) Linear combination fitting (red or gray circles) and the first derivative of the normalized $\mu(E)$ (black lines) of the μ-XANES of Sr^{2+} *K*-edge spectra for UA11PT1, UA13PT1, UA13PT2, UB1PT1, and UB1PT2. (b) The first derivative of the normalized $\mu(E)$ of the μ-XANES of Sr^{2+} *K*-edge spectra for the five standards used in the linear combination fitting.

Table 3. Linear Combination Fitting Results for Sr^{2+} *K*-edge μ-XANES Spectra in Figure 5a[a]

sample ID	Sr^{2+} ads. α-FeOOH (%)	Sr^{2+} ads. γ-FeOOH (%)	Sr^{2+} ads. $CaCO_3$ (%)	Sr^{2+} incorp. $CaCO_3$ (%)	R-factor (%)
		Chlorine Disinfection			
UA11 point 1	39.1	–	–	60.9	0.0196
UA13 point 1	16.2	–	–	83.8	0.0235
UA13 point 2	25.3	–	–	74.7	0.0004
		Chloramine Disinfection			
UB1 point 1	13.7	–	–	86.3	0.0633
UB1 point 2	7.00	–	93.0	0.00	0.0001

[a] Data presented as weighted percents (±10%) over the fit range of −20 to 80 eV.

drinking water within the distribution system. The UCMR also recognizes that erosion and/or dissolution of pipe deposits within the distribution system may affect human exposure levels.[7]

The present study determined that average concentrations of Sr^{2+} in the surface layers of iron corrosion products from four fully operational DWDS ranged from 3 to 54 mg kg^{-1}. The associated drinking waters all had Sr^{2+} concentrations <0.5 mg L^{-1}. No trend was observed between the Sr^{2+} water concentrations and the solids Sr^{2+} concentrations. On the basis of a strong preference for the Sr^{2+} to adsorb with $CaCO_3$, one might expect that the higher the Ca^{2+} concentration the higher the Sr^{2+} concentration in the solids but that was not the case with the sample set examined in this study.

The linear combination fit analysis for UA11 and UA13 indicated that 60 to 84% of the Sr^{2+} was substituting for Ca^{2+} in the M1 sites of $CaCO_3$ (Table 3). This finding was not unexpected because Sr^{2+} has a high affinity for binding or adsorbing to $CaCO_3$.[27−30] Calcite ($CaCO_3$) was detected in bulk XRD analysis and the drinking water for UA was at or near the calcite saturation index. 16 to 39% of the Sr^{2+}, however, was adsorbed to α-FeOOH (Table 3)—an unexpected result because the average point of zero charge of α-FeOOH is approximately 8.5[31] and the average drinking water pH of UA was 8.6 (Table 1). The overall surface charge of α-FeOOH in UA should, therefore, be neutral to slightly positive. Based on the work of Carroll et al.[32] and Sahai et al.,[33] it was surmized that Sr^{2+} was likely adsorbed to α-FeOOH by outer-sphere complexation.

Seven to thirteen percent of Sr^{2+} was adsorbed to α-FeOOH in the surface layer of sample UB. As in the case of the UA samples, Sr^{2+} was likely adsorbed by outer-sphere complexation (Points 1 and 2) (Table 3). The remaining 86% of Sr^{2+} was substituted for Ca^{2+} in the $CaCO_3$ structure at Point 1 and 93% of the Sr^{2+} was adsorbed to the surface of $CaCO_3$ grains at Point 2 (Table 3). The strong association of Sr^{2+} with $CaCO_3$ was surprising because $CaCO_3$ was not detected using bulk powder XRD in UB samples. The lack of distinguishable XRD diffraction peaks does not discount the presence of calcite. The relative abundance of calcite may have been below the detection limit for XRD (~5%). Additional support for the presence of calcite came from the UB water chemistry, which indicated that water in the distribution system exceeded the $CaCO_3$ saturation index (Table 1). Results from the XANES analysis demonstrated the importance of $CaCO_3$ in developing Sr^{2+} reservoirs in the surface layers of corrosion products.

Hydraulic disturbances such as scouring, flow reversals, and flushing[34,35] can dislodge corrosion product surface layers. Particulates, composed of iron and accessory phases and any associated metals, are then transported downstream and ultimately to consumer taps. Chemical disturbances resulting from changes to the water chemistry such as decreases in the concentrations of oxidants, for example, dissolved oxygen, chlorine, or chloramine, can cause reduction of Fe^{3+} to Fe^{2+}.[8,34−39] Iron(II) and any metals associated with the Fe^{3+}-phases, i.e. Sr^{2+}, would be released into the drinking water.[12]

This process weakens the integrity of iron corrosion product surface layers and can create particulates if hydraulically disturbed.

To examine the likelihood of Sr^{2+} migration from the surface layers of iron corrosion products toward consumers' taps, particulates from a filter inside a home fed by water from UA were examined. The average Sr^{2+} concentration of particulates was 40.26 mg kg^{-1}, approximately the same as the average Sr^{2+} concentration (38 mg kg^{-1}) in surface layers of the iron corrosion products from UA, suggesting that particulate-bound Sr^{2+} was detached from DWDS surfaces and was transported into a residence. The Sr^{2+} concentration of a drinking water sample collected at a tap in UA was 210 μg L^{-1}. Even though this concentration is lower than in the particulate, it is still orders of magnitude higher than the US EPA reporting threshold of the UCMR3 (0.3 μg L^{-1}).

Disturbances to iron drinking water pipe corrosion products typically cause red or discolored water episodes[40−44] during which consumers tend to avoid drinking the water. However, not all disturbances to surface layers of iron corrosion products produce a visible turbidity. Turbidity values below 5 nephelometric turbidity units can contain particulates that are not readily visible to consumers.[45]

Data presented in this paper are the first to quantify the potential for Sr^{2+} transport into drinking water. The data clearly demonstrated that drinking water with elevated Sr^{2+} concentrations and Sr^{2+}-rich particulates could reach consumer taps. Not only were Sr^{2+}-rich particulates moving into the home, but based on the Sr^{2+} concentration in the particulates, ingestion of only a small quantity would exceed the US EPA health reference level (HRL). The US EPA HRL for Sr^{2+} ingestion by a 70 kg adult is 4.20 mg kg^{-1}.[46] This value was based on the consumption of 2 L per day of drinking water with a relative Sr^{2+} contribution of 20% of the Sr^{2+} oral reference dose.

The implication of this study is that numerous DWDS have iron corrosion products with elevated Sr^{2+} concentrations. Also, the findings can be used as a start point to develop better a understanding of how modifications to water treatment strategies impact metal attenuation and amplification with corrosion products throughout drinking water distribution systems.

■ ASSOCIATED CONTENT

Ⓢ Supporting Information

Details on the strontium standard preparation, powder XRD patterns for the bulk samples from Utilities A−D from representative layers, iron and Sr^{2+} concentrations for representative layers of the iron corrosion products from all four utilities in Figure 3. This material is available free of charge via the Internet at http://pubs.acs.org.

■ AUTHOR INFORMATION

Corresponding Author

*Tel.: 01 513 556 3732. Fax: 01 513 556 6931. E-mail: Tammie.Gerke@uc.edu.

Notes

The authors declare no competing financial interest.

■ ACKNOWLEDGMENTS

PNC/XOR facilities at the Advanced Photon Source, and research at these facilities, are supported by the U.S. Department of Energy, Basic Energy Sciences, a major facilities access grant from NSERC, the University of Washington, Simon Fraser University, and the Advanced Photon Source. Use of the Advanced Photon Source was also supported by the U.S. Department of Energy, Office of Science, Office of Basic Energy Sciences, under Contract DE-AC02-06CH11357. MRCAT operations were supported by the Department of Energy and the MRCAT member institutions. This research has not been subject to Agency review and, therefore, does not necessarily reflect the views of the Agency. Mention of trade names of commercial products and companies does not constitute endorsement or recommendation for use. We thank M. R. Schock for his advice on improving the text, M. K. DeSantis for photographs of the iron corrosion products, and Mathew Jones for some sample preparation.

■ REFERENCES

(1) Dahl, S. G.; Allain, P.; Marie, P. J.; Mauras, Y.; Boivin, G.; Ammann, P.; Tsouderos, Y.; Delmas, P. D.; Christiansen, C. Incorporation and distribution of strontium in bone. *Bone* **2001**, *28* (4), 446−453.

(2) Eikenberga, J.; Triccab, A.; Vezzua, G.; Stilleb, P.; Bajoa, S.; Ruethi, M. ^{228}Ra/^{226}Ra/^{224}Ra and ^{87}Sr/^{86}Sr isotope relationships for determining interactions between ground and river water in the upper Rhine valley. *J. Environ. Radioact.* **2001**, *54*, 133−162.

(3) Langley, S.; Gault, A. G.; Ibrahim, A.; Takahashi, Y.; Renaud, R.; Fortin, D.; Clark, I. D.; Ferris, F. G. Sorption of strontium onto bacteriogenic iron oxides. *Environ. Sci. Technol.* **2009**, *43* (4), 1008−1014.

(4) Nielsen, S. P. The biological role of strontium. *Bone* **2004**, *35*, 583−588.

(5) Watts, P.; Howe, P. Strontium and Strontium Compounds. *Concise Int. Chem. Assess.* **2010**, *77*, 63.

(6) USEPA, Drinking Water Contamination Candidate List 3 Final Notice. In 2009; Vol. *74FR51850*, pp 51850-51862.

(7) US EPA. *Unregulated Contaminant Monitoring Rule 3* (UCMR 3); United States Environmental Protection Agency: Washington, DC, 2012; Vol. *77FR26071*, pp 26071−26101.

(8) Al-Jasser, A. O. Chlorine decay in drinking-water transmission and distribution systems: Pipe service age effect. *Water Res.* **2007**, *41* (2), 387−96.

(9) *Toxicological Profile for Strontium*; Agency for Toxic Substances and Disease Registry: Atlanta, GA, 2004.

(10) US EPA. *National Drinking Water Contaminant Occurrence Query User'S Guide. National Contaminant Occurrence Database*; US EPA: Washington, DC, 2002.

(11) Friedman, M. J.; Hill, A. S.; Reiber, S. H.; Valentine, R. L.; Larsen, G.; Young, A.; Korshin, G. V.; Peng, C. Y. *Assessement of Inorganics Accumulation in Drinking Water System Scales and Sediments*; Water Research Foundation: Denver, CO, 2010.

(12) Gerke, T. L.; Scheckel, K. G.; Maynard, J. B. Speciation and distribution of vanadium in drinking water iron pipe corrosion by-products. *Sci. Total Environ.* **2010**, *408*, 5845−5853.

(13) Triantafyllidou, S.; Parks, J.; Edwards, M. Lead Particles in Potable Water. *J. Am. Water Works Assoc.* **2007**, *99* (6), 107−117.

(14) Sarin, P.; Snoeyink, V. L.; Lytle, D. A.; Kriven, W. M. Iron corrosion scales: Model for scale growth, iron release and colored water formation. *J. Environ. Eng.* **2004**, *130*, 364−373.

(15) Cornell, R. M.; Schwertmann, U. *The Iron Oxides; Structure, Properties, Reactions, Occurrences and Uses*; Wiley-VCH Verlag GmbH & Co. KGaA: Darmstadt, 2003.

(16) Heald, S. M.; Brewe, D. L.; Stern, E. A.; Kim, K. H.; Brown, F. C.; Jiang, D. T.; Crozier, E. D.; Gordon, R. A. XAFS and micro-XAFS at the PNC-CAT beamlines. *J. Synch. Rad.* **1999**, *6*, 347−349.

(17) Kropf, A.; Katsoudas, J.; Chattopadhyay, S.; Shibata, T.; Lang, E.; Zyryanov, V.; Ravel, B.; McIvor, K.; Kemner, K.; Scheckel, K.; Bare, S.; Terry, J.; Kelly, S.; Bunker, B.; Segre, C. In *The New MRCAT (Sector 10) Bending Magnet Beamline at the Advanced Photon Source*

10th International Conference on Synchrotron Radiation Instrumentation, Melbourne, Australia, 2009; pp 299−302.

(18) Segre, C.; Leyarovska, N.; Chapman, L.; Lavender, W.; Plag, P.; King, A.; Kropf, A.; Bunker, B.; Kemner, K.; Dutta, P.; Duran, R.; Kaduk, J. In *The MRCAT insertion Device Beamline at the Advanced Photon Source, Synchrotron Radiation Instrumentation, Stanford, CA*; Pianetta, P.; Arthur, J.; Brennan, S., Eds.; Synchrotron Radiation Instrumentation: Stanford, CA, 1999; pp 419− 422.

(19) O'Day, P.; Newville, M.; Neuhoff, P.; Sahai, N.; Carrol, S. X-Ray absorption spectroscopy of strontium(II) coordination I. Static and thermal disorder in crystalline, hydrated, and precipitated solids and in aqueous solution. *J. Colloid Interface Sci.* **2000**, *222*, 184−197.

(20) Ravel, B.; Newville, M. ATHENA, ARTEMIS, HEPHAESTUS: Data analysis for X-ray absorption spectroscopy using IFEFFIT. *J. Synch. Rad.* **2005**, *12*, 537−541.

(21) Gerke, T. L.; Maynard, J. B.; Schock, M. R.; Lytle, D. A. Physiochemical characterization of five iron tubercles from a single drkinking water distribution system: Possible new insights on their formation and growth. *Corros. Sci.* **2008**, *50*, 2030−2039.

(22) Gerke, T. L.; Scheckel, K. G.; Ray, R. I.; Little, B. J. Can dynamic bubble templating play a role in corrosion product morphology? *Corrosion: J. Sci. Eng.* **2012**, *68* (2), DOI: 10.5006/1.3683226.

(23) Lin, J.; Ellaway, M.; Adrien, R. Study of corrosion material accumulated on the inner wall of steel water pipe. *Corros. Sci.* **2001**, *43* (11), 2065−2081.

(24) McNeill, L. S.; Edwards, M. Iron pipe corrosion in distribution systems. *J. Am. Water Works Assoc.* **2001**, *93* (7), 88−100.

(25) Tang, Z.; Hong, S.; Xiao, W.; Taylor, J. Characteristics of iron corrosion scales established under blending of ground, surface, and saline waters and their impacts on iron release in the pipe distribution system. *Corros. Sci.* **2006**, *48* (2), 322−342.

(26) Sancy, M.; Gourbeyre, Y.; Sutter, E. M. M.; Tribollet, B. Mechanism of corrosion of cast iron covered by aged corrosion products: Application of electrochemical impedance spectrometry. *Corros. Sci.* **2010**, *52* (4), 1222−1227.

(27) Finch, A. A.; Allison, N. Coordination of Sr and Mg in calcite and aragonite. *Mineral. Mag.* **2007**, *71* (5), 539−552.

(28) Shahwan, T.; Zunbul, B.; Akar, D. Study of the scavenging behavior and structural changes accompanying the interaction of aqueous Pb^{2+} and Sr^{2+} ions with calcite. *Geochem. J.* **2005**, *39* (4), 317−326.

(29) Parkman, R. H.; Charnock, J. M.; Livens, F. R.; Vaughan, D. J. A study of the interaction of strontium ions in aqueous solution with the surfaces of calcite and kaolinite. *Geochim. Cosmochim. Acta* **1998**, *62* (9), 1481−1492.

(30) Pingitore, N. E., Jr.; Lytle, F. W.; Davies, B. M.; Eastman, M. P.; Eller, P. G.; Larson, E. M. Mode of incorporation of Sr^{2+} in calcite: Determination by X-ray absorption spectroscopy. *Geochim. Cosmochim. Acta* **1992**, *56* (4), 1531−1538.

(31) Kosmulski, M. *Chemical Properties of Material Surface*; Marcel Dekker, Inc.: New York, 2001; Vol. *102*.

(32) Carroll, S. A.; Roberts, S. K.; Criscenti, L. J.; O'Day, P. A. Surface complexation model for strontium sorption to amorphous silica and goethite. *Geochem. Trans.* **2008**, *9*, 1−26.

(33) Sahai, N.; Carroll, S. A.; Roberts, S.; O'Day, P. A. X-ray absorption spectroscopy of strontium(II) coordination. II. Sorption and precipitation at kaolinite, amorphous silica, and goethite surfaces. *J. Colloid Interface Sci.* **2000**, *222* (2), 198−212.

(34) Sarin, P.; Snoeyink, V. L.; Bebee, J.; Jim, K. K.; Beckett, M. A.; Kriven, W. M.; Clement, J. A. Iron release from corroded iron pipes in drinking water distribution systems: Effect of dissolved oxygen. *Water Res.* **2004**, *38* (5), 1259−1269.

(35) Sung, W.; Huang, X.; Wei, I. W. Treatment and distribution system effects on chloramine decay, pH, nitrification, and disinfection by-products: Case study. *J. Water Res. Plan. Manage.* **2005**, *131* (3), 201−207.

(36) Lytle, D. A.; Sarin, P.; Snoeyink, V. L. The effect of chloride and orthophosphate on the release of iron from a cast iron pipe section. *J. Water Supply.: Res. Technol.—AQUA* **2005**, *54* (5), 267−281.

(37) Clark, R. M.; Yang, Y. J.; Impellitteri, C. A.; Haught, R. C.; Schupp, D. A.; Pangulluri, S.; Krishnan, E. R. Chlorine fate and transport in distribution systems: Experimental and modeling studies. *J. Am. Water Works Assoc.* **2010**, *102* (5), 144−155.

(38) Zhang, Y.; Edwards, M. Accelerated chloramine decay and microbial growth by nitrification in premise plumbing. *J. Am. Water Works Assoc.* **2009**, *101* (11), 51−62.

(39) Westbrook, A.; Digiano, F. A. Rate of chloramine decay at pipe surfaces. *J. Am. Water Works Assoc.* **2009**, *101* (7), 59−70.

(40) Wang, H.; Hu, C.; Hu, X.; Yang, M.; Qu, J. Effects of disinfectant and biofilm on the corrosion of cast iron pipes in a reclaimed water distribution system. *Water Res.* **2012**, *46* (4), 1070−1078.

(41) Husband, P. S.; Boxall, J. B.; Saul, A. J. Laboratory studies investigating the processes leading to discolouration in water distribution networks. *Water Res.* **2008**, *42*, 4309−4318.

(42) Matsui, Y.; Yamagishi, T.; Terada, Y.; Matsushita, T.; Inoue, T. Suspended particles and their characteristics in water mains: development of sampling methods. *J. Water Supply: Res. Technol.—AQUA* **2007**, *56* (1), 13−24.

(43) Polychronopolous, M.; Dudley, K.; Ryan, G. J. H. Investigation of factors contributing to dirty water events in reticulation systems and evaluation of flushing methods to remove deposited particles: A review. *Water Sci. Technol.: Water Supply* **2003**, *3* (1−2), 295−306.

(44) Vreeburg, J. H.; Boxall, J. B. Discoloration in potable water distribution systems: A review. *Water Res.* **2007**, *41* (3), 519−29.

(45) US EPA. *National Primary Drinking Water Regulations*; US EPA: Washington, DC, 2009; EPA 816-F-09-0004.

(46) US EPA. *Contaminant Information Sheets for the Final CCL 3 Chemicals*; US EPA: Washington, DC, 2009; EPA 815-R-09-012, p 214.

(47) Baylis, J. R. Prevention of corrosion and red water. *J. Am. Water Works Assoc.* **1926**, *15*, 598−633.

(48) Rossmann, R.; Barres, J. Trace element concentrations in near-surface waters of the Great Lakes and methods of collection, storage, and analysis. *J. Great Lakes Res.* **1988**, *14* (2), 188−204.